ACS OMEGA

Article

Cite This: ACS Omega 2018, 3, 159−166

Noncovalent Approach to Liquid-Crystalline Ion Conductors: High-Rate Performances and Room-Temperature Operation for Li-Ion Batteries

Taira Onuma,[†] Eiji Hosono,*[,‡] Motokuni Takenouchi,[†] Junji Sakuda,[†] Satoshi Kajiyama,[†] Masafumi Yoshio,[†,§] and Takashi Kato*[,†]

[†]Department of Chemistry and Biotechnology, School of Engineering, The University of Tokyo Hongo, Bunkyo-ku, Tokyo 113-8656, Japan

[‡]Research Institute for Energy Conservation, National Institute of Advanced Industrial Science and Technology, Umezono, Tsukuba, Ibaraki 305-8568, Japan

Supporting Information

ABSTRACT: We report advanced liquid-crystalline (LC) electrolytes for use in lithium-ion batteries (LIBs). We evaluated the potential of LC electrolytes with a half cell composed of Li metal and $LiFePO_4$ which is a conventional positive electrode for LIBs. Low-molecular-weight carbonates of ethylene carbonate or propylene carbonate were incorporated into the two-dimensional (2D) nanostructured electrolyte composed of mesogen-containing carbonate and lithium bis(trifluoromethylsulfonyl)imide. The incorporation of low-molecular-weight carbonates increased the ionic conductivity with maintaining 2D nanostructures in the LC state. High-power performances at relatively high current densities induced by higher ionic conductivities have been achieved by LC electrolytes with low-molecular-weight carbonates. Furthermore, room-temperature operation of LIBs using LC electrolytes is reported for the first time. In the research field of electrolytes for LIBs, we demonstrate the progress of a new category of LC electrolytes.

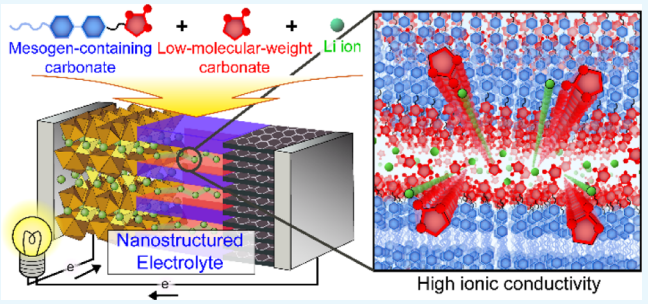

INTRODUCTION

Intensive studies have focused on ion-transport solid and quasisolid organic materials[1−5] for the development of actuators,[6] transistors,[7] electrochromic devices,[8,9] water-treatment membranes,[10−13] and in particular, energy devices such as batteries[14−16] and capacitors[15,17,18] because solid organic materials have light-weight properties, easy processability, and film-forming abilities. These properties are advantageous for versatile and large-scale applications, especially for portable and flexible electronics. Gel polymers,[19−21] solid polymers,[22−25] ionic plastic crystals,[26−28] and nanostructured liquid crystals[29−32] have been developed as organic ion transporters for applications as electrolytes. Recently, ion-conductive liquid crystals[29−40] and ionic solids preserving liquid-crystalline (LC) structures[41−45] have attracted attention as quasisolid and solid-state electrolytes because they provide 1D,[33,34] 2D,[35−37] and 3D[38−40] nanochannels. These materials are expected to act as efficient and selective ion transporters. There are two types of LC electrolytes. One type is polar liquid crystals complexed with ionic species. For example, poly- and oligo-oxyethylene[35] and carbonates[33,36] have been used to form the complexes. The other type is ionic liquid crystals, which contain imidazolium,[34,37] ammonium,[38] phosphonium,[38] and sulfonate ions.[39,40] These materials also show miscible properties with ionic salts.

Energy-generating and energy-storage devices have been developed based on the accumulated results of the basic research on LC ion conductors.[33−45] For energy-generating devices, dye-sensitized solar cells (DSSCs) using LC electrolytes have been fabricated.[46−51] We successfully applied carbonate-based liquid crystals complexed with ionic liquids and iodides for DSSCs. Thermally stable DSSCs were obtained by using 2D nanostructured LC complexes as electrolytes transporting I^-/I_3^- species. These solar cells can be operated at remarkably high temperatures up to 120 °C owing to the nonvolatile and thermally stable properties of the LC electrolytes.[46−51] Improvement of the durability under high temperature conditions is an important problem to be solved in the research of DSSCs. The possibility for the use in DSSCs was demonstrated by exploiting the characteristics of LC electrolytes.

Our strategy is to construct LIBs based on LC electrolytes in the field of energy storage. LIBs are suitable for electric vehicles

Received: October 7, 2017
Accepted: December 22, 2017
Published: January 5, 2018

DOI: 10.1021/acsomega.7b01503
ACS Omega 2018, 3, 159−166

and plug-in electric vehicles because of the high energy densities. Intensive research has focused on the high-power performance and high energy density of LIBs.[52−55]

Among the research and development issues for LIBs, the electrolyte is an important factor in addition to the active materials of the cathode and anode because there are strong correlations between the electrolyte and the properties of power, charge−discharge cycles, and safety. Organic electrolytic solutions, which are practically used in the current LIBs, have a safety problem owing to their high volatility, flammability, and potential for leakage.[56−58] Safer electrolytes are urgently required. Solid-state and quasisolid-state alternatives have attracted growing interest in place of liquid electrolytes.[59−64]

For the first time, we reported smectic LC electrolytes for LIBs.[64] As electrolytes for LIBs, materials with a high resistivity against degradation caused by the high oxidation and low reduction potentials are important. This was an essential problem to be solved for liquid crystals for the application to LIBs. We designed and prepared rod-shaped molecule **1** having a mesogenic moiety and a cyclic carbonate moiety at the terminal of the alkyl chain spacer.[64] The mixtures of **1** and Li salts were operated as an LC electrolyte for LIBs at 60 °C. Reversible charge−discharge was observed for the LIBs composed of the LC electrolytes.[64] In spite of the high expectation of LC electrolytes, high-rate performance LIBs based on LC electrolytes have not yet been achieved owing to the problems of ionic conductivities. Higher ionic conductivities of LC electrolytes were required for the development of high-power LIBs with room-temperature operation. We previously reported an enhancement of ionic conductivity by a noncovalent approach.[65,66] The use of noncovalent interactions such as hydrogen bonding and ion−dipole/dipole−dipole interactions enables supramolecular organization of mobile molecules into LC nanostructures.[39,44,45,65,66] For example, mesogenic molecules having hydroxy groups mixed with ionic liquids form layered[65] and cylindrical[66] nanochannels of ionic liquids as conducting LC self-assemblies through hydrogen bonding interactions between hydroxy groups and ionic liquids. For the construction of efficient Li-ion conductors, Gin et al. reported the polymerized lyotropic LC systems with 3D interconnected nanopores filled with Li-salt-doped organic carbonate liquid electrolytes.[44,45] 1D and 3D Li-ion conductors composed of zwitterionic liquid crystals, an Li salt, and a carbonate electrolyte were developed in our previous work.[39] In these systems, carbonate electrolytes play important roles both in enhancement of ionic conductivity by improving dissociation of Li salts and mobility of ions and in formation of nanosegregated LC structures through ion−dipole interactions between Li-ions and carbonate molecules. Thus, incorporation of mobile small electrolyte molecules into the LC ion-conductive nanostructures can be a promising strategy to obtain highly conductive materials for LIBs.

In the present study, to achieve high performance for LIBs with LC electrolytes, we have applied ternary mixtures of compound **1**, lithium bis(trifluoromethylsulfonyl)imide (LiTFSI), and ethylene carbonate (EC) or propylene carbonate (PC) (Figure 1). We expected that EC or PC molecules would be incorporated into the self-organized structure with structure-directing molecule **1** through weak noncovalent interactions. The ternary mixtures are expected to form highly Li-ion-conductive 2D pathways, resulting in the construction of high-performance LIBs (Figure 2). We discuss the potential of the LC electrolytes on the basis of electrochemical performance of

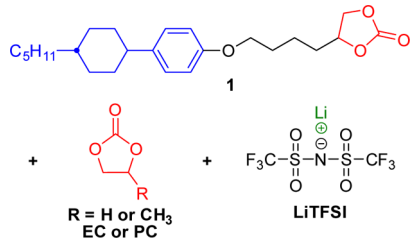

Figure 1. Chemical structures of the components of the electrolytes.

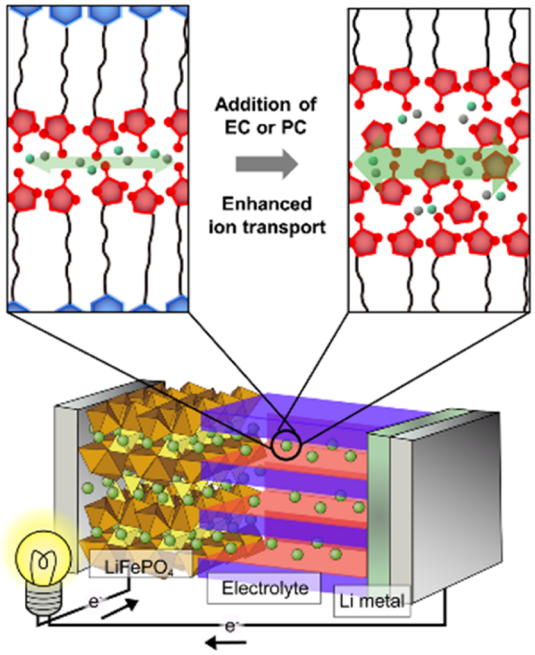

Figure 2. Schematic illustration of the strategy in the present study to enhance the ion conductivities for Li-ion transport in the nanostructured LC electrolyte for the lithium-ion battery (LIB).

half cells composed of Li metal and $LiFePO_4$ which is a conventional positive electrode material for LIBs.

RESULTS AND DISCUSSION

LC Properties. Ternary mixtures of compound **1**, EC or PC, and LiTFSI were prepared. The molar ratio of LiTFSI was maintained at 10 mol % for the mixtures. We previously observed that the ionic conductivities at 10 mol % of LiTFSI became a maximum for the binary mixtures of **1** and LiTFSI.[64]

Table 1 presents the phase transition behavior of the ternary mixtures as a function of the weight ratio of EC in the mixture of **1**, EC, and LiTFSI. These components were miscible, and their mixtures showed stable smectic A (SmA) phases (Supporting Information, Figures S1 and S2) in a wide range of temperatures. The isotropization temperatures of the mixtures decreased as the weight ratio of EC increased. For example, the SmA isotropic transition was observed at 114 °C for the binary mixtures of **1** and LiTFSI, whereas the isotropization temperature was observed at 80 °C for the ternary mixtures of **1**, LiTFSI, and EC of 29 wt % [**1**/EC(29)]. This behavior can be explained by the destabilization of layered structures by the introduction of smaller molecules as is observed in other LC systems.[39] The wide-angle X-ray diffraction (XRD) pattern for **1**/EC(29) at 60 °C showed three reflection peaks at 49.1, 25.6, and 16.3 Å corresponding

DOI: 10.1021/acsomega.7b01503
ACS Omega 2018, 3, 159−166

Table 1. Phase Transition Behavior of the Mixtures of Compound 1, EC or PC, and LiTFSI (10 mol %) on Cooling[a]

sample[b]	phase transition behavior[c]				
1 + LiTFSI	Iso	114	SmA	0	SmB
1/EC(8)	Iso	102	SmA		
1/EC(16)	Iso	99	SmA		
1/EC(29)	Iso	80	SmA		
1/PC(32)	Iso	53	SmA		

[a]Iso: isotropic; SmA: smectic A; SmB: smectic B. [b]Ratio of EC or PC is indicated as follows: **1**/EC(x) or **1**/PC(x), where x indicates the wt % of EC or PC in each electrolyte. [c]Determined by differential scanning calorimetry at the rate of 10 °C min^{-1} on cooling.

to the (001), (002), and (003) reflections, respectively, of a layered structure with a spacing of approximately 50 Å (Figure S3). The layer spacing was nearly twice the molecular length of **1**, which was estimated to be 22 Å by molecular mechanics calculations. This observation indicated the formation of a bilayer structure in the SmA phase. The interlayer spacings of the smectic structures were examined for the mixtures of different weight ratios of EC at 60 °C (Figure S4). The spacings increased as the weight ratio of EC increased. These results suggest that the EC molecules were organized into the bilayer structures as shown in Figure 2. The ternary mixture of **1**, LiTFSI, and PC of 32 wt % (**1**/PC(32)), in which the molar content of PC was the same as that of EC in **1**/EC(29), also showed the SmA phase, and its isotropization temperature was 27 °C lower than that of **1**/EC(29).

Ionic Conductivities. Ionic conductivities of the mixtures were measured by the alternating current impedance method using the cells with comb-shaped gold electrodes on a glass substrate. Figure 3 shows the ionic conductivities of the LC

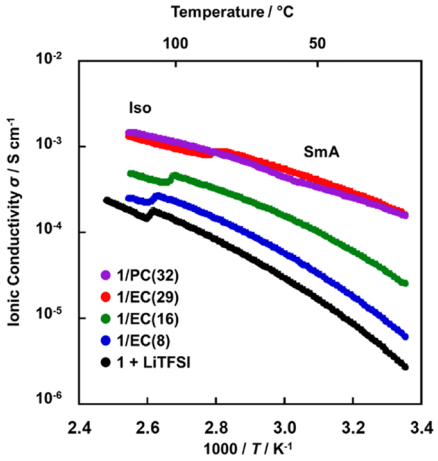

Figure 3. Ionic conductivities of the mixtures of **1**, EC or PC, and LiTFSI on heating.

mixtures. All the ionic conductivities were measured on the heating processes preceded by the isotropization of the samples and the cooling to room temperature. All the samples were homeotropically aligned in the smectic phases on the glass substrates. At the smectic−isotropic phase transitions, an abrupt decrease in the conductivities was observed. These trends suggested that the 2D ionic pathways in the smectic structures were disrupted because of the phase transition to the isotropic phase. The higher EC content led to the higher ionic conductivities. The conductivities of the ternary mixtures of **1**/EC(29), **1**/EC(16), and **1**/EC(8) at 60 °C were 5.5 × 10^{-4}, 1.7 × 10^{-4}, and 5.7 × 10^{-5} S cm^{-1}, respectively. Compared with the conductivities of the binary mixture of **1** and LiTFSI, the ternary mixtures showed higher conductivities. The conductivities of **1**/EC(29) at 60 and 25 °C were approximately 20 times and 60 times higher than those of the binary mixture, respectively. For the ternary mixture, highly mobile EC molecules efficiently transported Li-ions within the conducting layers of the smectic structures. The conductivities of **1**/PC(32) were almost the same as those of **1**/EC(29) in spite of the difference of isotropization temperatures.

High-Power Performance for LIBs. The electrochemical stability of the LC electrolyte of **1**/EC(29) was evaluated by the cyclic voltammetry (CV) measurements of a coin-type cell constructed by a working electrode of stainless steel and a counter electrode of Li metal. A cyclic voltammogram in the potential range of −0.04 to 3.9 V versus Li/Li$^+$ at 60 °C at a scan rate of 0.025 mV s^{-1} showed peaks of lithium deposition and dissolution at approximately 0 V versus Li/Li$^+$. No significant peaks by decomposition in the potential range up to 3.9 V versus Li/Li$^+$ were observed. These results suggest that these LC electrolytes can be applied to LIBs with a wide potential range.

The rate capabilities of the LC electrolytes prepared in the present study were evaluated by charging and discharging the $LiFePO_4$ positive electrode for successive 5 × 5 cycles at current rates of 5, 25, 100, and 500 mA g^{-1} and then back to 5 mA g^{-1} at 60 °C (Figure 4). It is noteworthy that the initial (1st

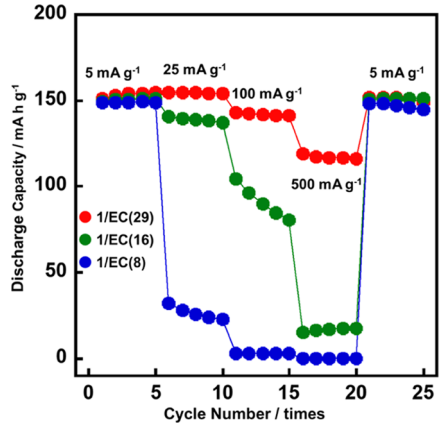

Figure 4. Rate performances of the cells composed of Li/LC electrolyte/$LiFePO_4$ with the electrolytes of **1**/EC(29), **1**/EC(16), and **1**/EC(8) in the potential range of 2.7−3.8 V vs Li/Li$^+$ for successive 5 × 5 cycles at rates of 5, 25, 100, and 500 mA g^{-1}, and then back to 5 mA g^{-1} at 60 °C.

cycle) and final (25th cycle) capacities of approximately 150 mA g^{-1} at a low current density of 5 mA g^{-1} were near to the theoretical capacity of $LiFePO_4$ (172 mA h g^{-1}). In addition, in the case of **1**/EC(29), for example, initial and final capacities were almost the same values of 151 and 149 mA h g^{-1}, that is, 98.7% of capacity was retained, while ca. one month passed during the start and the end of the measurements. These results suggest that the LC electrolytes have sufficient long-term stability, and no significant side reactions stemmed from the electrolyte components occur during the operation in LIBs. These results indicate that the LC electrolytes can function as an electrolyte of LIBs. Notably, in the case of **1**/EC(29), the

DOI: 10.1021/acsomega.7b01503
ACS Omega 2018, 3, 159−166

capacity of 154 mA h g^{-1} was retained at a current density of 25 mA g^{-1}. Moreover, the capacity was still retained at high values of 142 and 117 mA g^{-1} even at relatively high current densities of 100 and 500 mA g^{-1}, respectively. This excellent rate performance for the LC electrolytes arose from the high ionic conductivity as shown in Figure 3. These results suggest that the novel LC electrolytes formed through the noncovalent approach achieved an improvement of the high-power performances of LIBs using the LC electrolyte.

The electrolyte of **1**/EC(16) retained a capacity of 140 mA h g^{-1} at a current density of 25 mA g^{-1}. However, the capacity decreased to 96 and 16 mA h g^{-1} at relatively high current densities of 100 and 500 mA g^{-1}, respectively. In the electrolyte of **1**/EC(8), the capacity was 28 mA h g^{-1} even at a relatively low current density of 25 mA g^{-1}. The capacity was not observed at high current densities of 100 and 500 mA g^{-1}. These properties resulted from the ratio of EC in the mixture that significantly affects the ionic conductivities, as shown in Figure 3.

The charge/discharge profiles at different current densities are presented in Figure 5. The potential plateaus of the charge/discharge profiles by **1**/EC(29) show a small polarization at a current density of up to 100 mA g^{-1}, suggesting low resistance of the LC electrolyte. The polarization of the potential plateau was still small even at a high current density of 500 mA g^{-1}. These results suggest that the Li-ion diffusion rate in the LC electrolyte of **1**/EC(29) was sufficient for the charge−discharge reaction up to the current rate of 500 mA g^{-1}. In the electrolyte of **1**/EC(16), the potential plateaus of the charge/discharge profiles showed a plateau even at a current density of 100 mA g^{-1}. The extent of polarization was similar to that of **1**/EC(29) at a high current density of 500 mA g^{-1}. The plateaus and capacity were almost not observed at a current density of 500 mA g^{-1}. The plateaus were only observed at a low current density of 5 mA g^{-1} in the electrolyte of **1**/EC(8). These differences of polarization and capacity were caused by the resistance components. For the resistance components of LIBs, the different values of ionic conductivities of the LC electrolytes caused the differences in the resistance of these cells. The rate capabilities, capacities, and polarization of potential plateaus were related to the ionic conductivity of each electrolyte. The electrolyte of **1**/EC(29), exhibiting the highest ionic conductive properties, showed the smallest polarization and the most stable plateau, which resulted in the highest power performance of LIBs.

Room-Temperature Operation of LIBs. Because the operation of LIBs at room temperature is important for the development of electrolytes, we have examined the performance of LIBs with the ternary mixtures of the LC electrolytes, **1**/EC(29) and **1**/PC(32).

Figure 6 shows the charge−discharge profiles and the rate capabilities of the $LiFePO_4$ positive electrode for various current rates at 25 °C. **1**/EC(29) and **1**/PC(32) show capacities of 138 and 136 mA h g^{-1} at a low current density of 5 mA g^{-1}, respectively. **1**/EC(29) with a high ionic conductivity retains high values of 126 and 100 mA h g^{-1} at 25 and 100 mA g^{-1}, respectively. The high-rate performance of **1**/PC(32) was similar to that of **1**/EC(29). The charge−discharge curves of **1**/EC(29) and **1**/PC(32) in Figure 7 showed a similar behavior, where the flat plateaus with small polarization appeared at moderate current rates of 5 and 25 mA g^{-1}. It should be noted that the noncovalent approach to the formation of the LC electrolytes for LIBs is effective for the enhancement of the LIB performance, leading to the achievement of room-temperature operation.

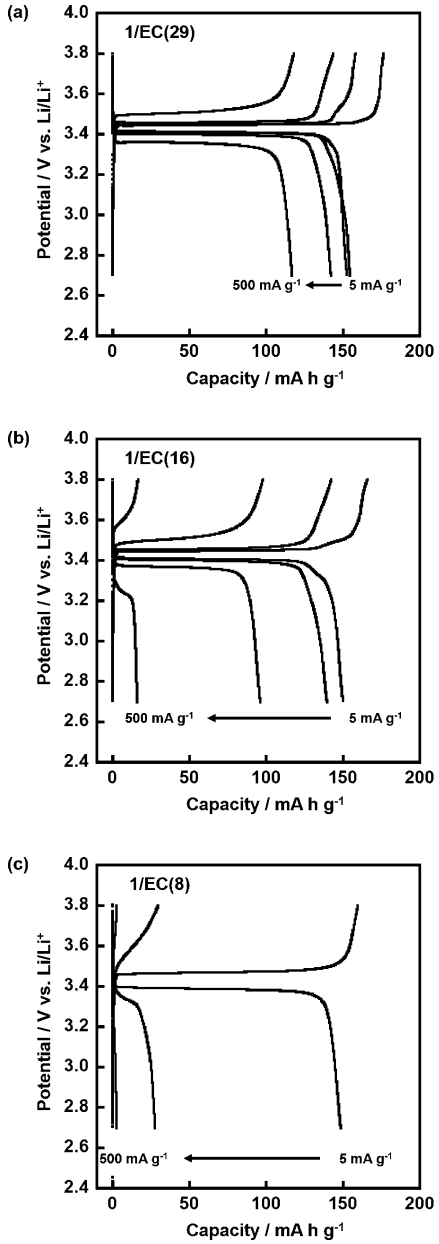

Figure 5. Charge−discharge profiles of the cells composed of Li/LC electrolyte/$LiFePO_4$ with the electrolytes of (a) **1**/EC(29), (b) **1**/EC(16), and (c) **1**/EC(8) in the potential range of 2.7−3.8 V vs Li/Li^+ for successive 5 × 5 cycles at rates of 5, 25, 100, and 500 mA g^{-1} at 60 °C. The curves correspond to the 2nd cycles at each rate (2nd, 7th, 12th, and 17th cycles in Figure 4).

We compared the rate capabilities between our LC electrolyte of **1**/EC(29) in the current study with polymer electrolytes[67−70] to emphasize the excellent performance of the LIBs with the LC electrolytes prepared through the noncovalent approach (Figure 8). Figure 8 shows the relationships between the capacity of an $LiFePO_4$ electrode and the current density of the present LC electrolyte of **1**/EC(29), other polymer electrolytes of BAB triblock copolymers,[67] block copoly(ionic liquid)s,[68] composite of PEO-$LiClO_4$ with ZrO_2,[69] and polysiloxane-based polymers[70] at various temperatures. The capacity of the LC electrolyte of **1**/EC(29) at 60 °C

DOI: 10.1021/acsomega.7b01503
ACS Omega 2018, 3, 159−166

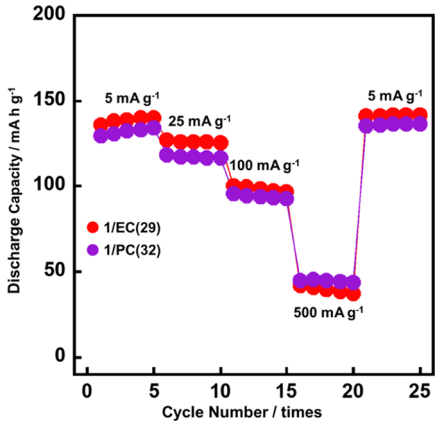

Figure 6. Rate performances of the cells composed of Li/LC electrolyte/$LiFePO_4$ with the electrolytes of **1**/EC(29) and **1**/PC(32) in the potential range of 2.7−3.8 V vs Li/Li^+ for successive 5 × 5 cycles at rates of 5, 25, 100, and 500 mA g^{-1}, and then back to 5 mA g^{-1} at 25 °C.

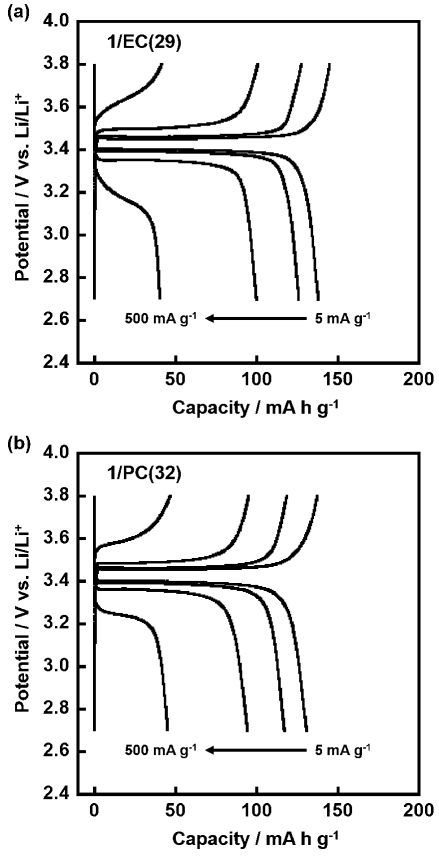

Figure 7. Charge−discharge profiles of the cells composed of Li/LC electrolyte/$LiFePO_4$ with the electrolyte of (a) **1**/EC(29) and (b) **1**/PC(32) in the potential range of 2.7−3.8 V vs Li/Li^+ for successive 5 × 5 cycles at rates of 5, 25, 100, and 500 mA g^{-1} at 25 °C. The curves correspond to the 2nd cycles at each rate (2nd, 7th, 12th, and 17th cycles in Figure 6).

exhibited a rate capability similar to that of the BAB triblock copolymer[67] and the polysiloxane-based polymer[68] at 60 °C. At a room temperature of 25 °C, both the LC electrolyte of **1**/EC(29) and the polysiloxane-based polymer[68] exhibited a comparable rate capability. The performance of the block copoly(ionic liquid)s[70] at 70 °C was lower than that of the LC

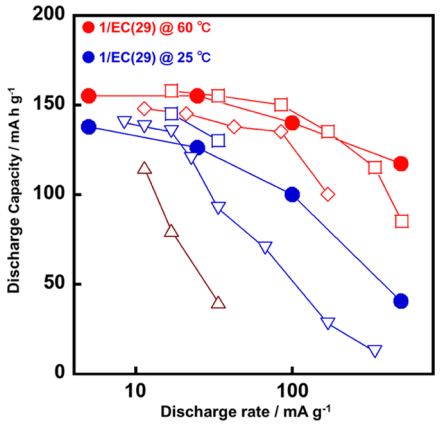

Figure 8. Capacity of the $LiFePO_4$ electrode vs the current density of the LC electrolyte of **1**/EC(29) at 60 °C (red circle) and 25 °C (blue circle), polymer electrolytes of BAB triblock copolymers[67] at 60 °C (red diamond), polysiloxane-based polymers[68] at 60 °C (red square) and 25 °C (blue square), composite of PEO-$LiClO_4$ with ZrO_2[69] at 25 °C (blue nabla), and block copoly(ionic liquid)s[70] at 70 °C (brown triangle).

electrolyte of **1**/EC(29) even at 25 °C. In the comparison between the LC electrolyte of **1**/EC(29) with the composite polymer electrolyte of PEO-$LiClO_4$ with ZrO_2[69] at 25 °C, a similar behavior of the rate capability was shown up to a current density of 25 mA g^{-1}. In the region of a current density over 25 mA g^{-1}, the LC electrolyte of **1**/EC(29) showed higher power and energy density. Therefore, the LC electrolyte of **1**/EC(29) exhibited a comparable performance with the polymer electrolytes at 60 °C and at room temperature. A further improvement of the design for the LC electrolytes in LIBs through noncovalent approaches would realize a much higher performance.

CONCLUSIONS

LC electrolytes constructed by mesogen-containing carbonate, LiTFSI, and low-molecular-weight electrolytes of EC or PC have exhibited high-power performances at 60 °C. Furthermore, we demonstrate room-temperature operation of the LIBs by using the LC electrolytes for the first time. The addition of low-molecular-weight carbonates into the 2D LC structures enhances the ionic conductivity at various temperature regions, including room temperature, and improves the rate performance of the LIBs. The improvement of ionic conductivities, which has been achieved through the noncovalent approach in an LC system, leads to the high-power performances and room-temperature operation of the LIBs. These results of the LC electrolytes propose that they are a new category of energy materials with high performances and stability.

EXPERIMENTAL SECTION

General Procedures. The phase-transition behavior of the mixtures was investigated by differential scanning calorimetry (DSC) (Netzsch DSC204 Phoenix calorimeter) with the cooling/heating rates of 10 K min^{-1}. Transition temperatures were recorded at the onset of the transition peaks on first cooling. The LC properties were examined by a polarizing optical microscope (Olympus BX53) with a heating stage (Linkam LTS 350). XRD was measured by a diffractometer (Rigaku RINT-2500) using a Cu Kα line. Molecular mechanics

DOI: 10.1021/acsomega.7b01503
ACS Omega 2018, 3, 159−166

calculations were conducted on the Wavefunction SPARTAN'10 (v. 1.1.0) program.

Materials. All the chemicals used for the preparation of compound **1** were purchased from commercial sources and used without purification. LiTFSI and EC of a lithium battery grade were purchased from Kishida Chemical, and PC of an electrochemical grade was purchased from Kanto Chemical Co., Inc. Compound **1** was synthesized according to the previously reported procedures.[18]

Preparation of the Ternary Mixtures of 1, EC or PC, and LiTFSI. Prior to preparing ternary mixtures of the LC electrolytes, the binary mixtures of compound **1** and LiTFSI were prepared by dissolving the components in tetrahydrofuran followed by slow evaporation of the solvent at 80 °C under a reduced pressure in a vacuum oven. After that, EC or PC was added to the binary mixtures of **1** and LiTFSI in an argon-filled glovebox. The containers of these mixtures were tightly sealed and heated to 120 °C. After the mixtures were homogenized in the isotropic states, they were cooled to room temperature.

Measurements of Ionic Conductivities. The ionic conductivities were measured by the alternating current impedance method using a chemical impedance meter (HIOKI 3532-80) (frequency range: 100 Hz to 1 MHz, applied voltage: 0.3 V) with a heating stage (Linkam LTS 350), a temperature controller (Linkam TMS 94), and a hot-stage cooler (Linkam LNP 9412) with the heating rate of 2 K min^{-1}. Ionic conductivities were calculated to be the product of $1/R_b$ (Ω^{-1}) times the cell constants (cm^{-1}) for comb-shaped gold electrodes with SiO_2 microparticle spacers (16 μm), which were calibrated with the HI7033L 84 μS cm^{-1} conductivity standard from Hanna Instruments.

Cyclic Voltammetry. CR2032-type coin cells were assembled in an argon-filled glovebox using a stainless-steel plate (SUS-316L) as the working electrode and Li metal as the counter electrode. A polypropylene film was used as a separator, which was filled with the LC electrolytes. The electrolytes were spread on the separators prior to the assembly of the cells. The assembled cells were placed in a thermostat at 120 °C for 15 min to allow the separators to soak up the electrolytes. The CV was measured on a BioLogic VMP3 Multichannel potentiostat within the potential range of −0.04 to 3.9 V versus Li/Li^+ at a scan rate of 0.025 mV s^{-1} at 60 °C.

Charge−Discharge Experiments. The powder of $LiFePO_4$ (SLFP-PT30, Tatung Fine Chemical) as the active material, carbon black (Super P-Li, TIMCAL) as an electrically conductive additive, and poly(vinylidene difluoride) (PVDF#1300, Kureha) as a binder were mixed in *N*-methyl-2-pyrrolidone with an ultrasonic homogenizer (UH-50, SMT Co., Ltd.) to obtain the slurry of the electrode material. The weight ratio of the solid materials was 65:30:5. The $LiFePO_4$ electrode was prepared by spreading the slurry onto an Al-foil as a current collector. The slurry was dried at 100 °C in a vacuum oven for 90 min. CR2032-type coin cells were assembled in an argon-filled glovebox using Li metal as the reference and counter electrode. A polypropylene film was used as a separator, which was filled with the LC electrolytes. The electrolytes were spread on the separators prior to the assembly of the cells. The assembled cells were placed in a thermostat at 120 °C for 15 min for the separators to soak up the electrolytes. Galvanostatic charge−discharge cycling of the $LiFePO_4$ electrode was tested on a Hokuto Denko galvanostat in the potential range of 2.7 to 3.8 V versus Li/Li^+ for 5 cycles at rates of 5, 25, 100, and 500 mA g^{-1}, and then back to 5 mA g^{-1} at 60 °C. The specific current and the specific capacity were calculated on the basis of the weight of the composite.

■ ASSOCIATED CONTENT

Supporting Information

The Supporting Information is available free of charge on the ACS Publications website at DOI: 10.1021/acsomega.7b01503.

LC properties of the mixtures of compound **1**, EC, and LiTFSI, including a polarizing optical microscopic image, DSC thermograms, and X-ray diffraction studies; cyclic voltammogram of **1**/EC(29) (PDF)

■ AUTHOR INFORMATION

Corresponding Authors

*E-mail: e-hosono@aist.go.jp (E.H.).
*E-mail: kato@chiral.t.u-tokyo.ac.jp (T.K.).

ORCID

Taira Onuma: 0000-0002-7878-5675
Satoshi Kajiyama: 0000-0002-2200-7524
Masafumi Yoshio: 0000-0002-1442-4352
Takashi Kato: 0000-0002-0571-0883

Present Address

§Research Center for Functional Materials, National Institute for Materials Science (NIMS) Sengen, Tsukuba-city Ibaraki 305-0047 Japan (M.Y.).

Notes

The authors declare no competing financial interest.

■ ACKNOWLEDGMENTS

This study was partially supported by CREST (Core Research for Evolutional Science and Technology) (JPMJCR1422) of Japan Science and Technology Agency (JST). T.O. was supported by Japan Society for the Promotion of Science through the Program for Leading Graduate Schools (MERIT).

■ REFERENCES

(1) Kato, T.; Yoshio, M.; Ichikawa, T.; Soberats, B.; Ohno, H.; Funahashi, M. Transport of Ions and Electrons in Nanostructured Liquid Crystals. *Nat. Rev. Mater.* **2017**, *2*, 17001.

(2) Kato, T.; Mizoshita, N.; Kishimoto, K. Functional Liquid-Crystalline Assemblies: Self-Organized Soft Materials. *Angew. Chem., Int. Ed.* **2006**, *45*, 38−68.

(3) Zheng, Y.; Lui, J.; Ungar, G.; Wright, P. V. Solvent-Free Low-Dimensional Polymer Electrolytes for Lithium-Polymer Batteries. *Chem. Rec.* **2004**, *4*, 176−191.

(4) Goossens, K.; Lava, K.; Bielawski, C. W.; Binnemans, K. Ionic Liquid Crystals: Versatile Materials. *Chem. Rev.* **2016**, *116*, 4643−4807.

(5) Mansueto, M.; Laschat, S. Ionic Liquid Crystals. In *Handbook of Liquid Crystals*, 2nd ed.; Goodby, J. W., Collings, P. J., Kato, T., Tschierske, C., Gleeson, H., Raynes, P., Eds.; Wiley-VCH: Weinheim, 2014; Vol. *6*, pp 231−280.

(6) Duncan, A. J.; Leo, D. J.; Long, T. E. Beyond Nafion: Charged Macromolecules Tailored for Performance as Ionic Polymer Transducers. *Macromolecules* **2008**, *41*, 7765−7775.

(7) Kim, S. H.; Hong, K.; Xie, W.; Lee, K. H.; Zhang, S.; Lodge, T. P.; Frisbie, C. D. Electrolyte-Gated Transistors for Organic and Printed Electronics. *Adv. Mater.* **2013**, *25*, 1822−1846.

(8) Thakur, V. K.; Ding, G.; Ma, J.; Lee, P. S.; Lu, X. Hybrid Materials and Polymer Electrolytes for Electrochromic Device Applications. *Adv. Mater.* **2012**, *24*, 4071−4096.

DOI: 10.1021/acsomega.7b01503
ACS Omega 2018, 3, 159−166

(9) Yazaki, S.; Funahashi, M.; Kato, T. An Electrochromic Nanostructured Liquid Crystal Consisting of π-Conjugated and Ionic Moieties. *J. Am. Chem. Soc.* **2008**, *130*, 13206−13207.
(10) Broer, D. J.; Bastiaansen, C. M. W.; Debije, M. G.; Schenning, A. P. H. J. Functional Organic Materials Based on Polymerized Liquid-Crystal Monomers: Supramolecular Hydrogen-Bonded Systems. *Angew. Chem., Int. Ed.* **2012**, *51*, 7102−7109.
(11) Henmi, M.; Nakatsuji, K.; Ichikawa, T.; Tomioka, H.; Sakamoto, T.; Yoshio, M.; Kato, T. Self-Organized Liquid-Crystalline Nanostructured Membranes for Water Treatment: Selective Permeation of Ions. *Adv. Mater.* **2012**, *24*, 2238−2241.
(12) Bögels, G. M.; van Kuringen, H. P. C.; Shishmanova, I. K.; Voets, I. K.; Schenning, A. P. H. J.; Sijbesma, R. P. Selective Absorption of Hydrophobic Cations in Nanostructured Porous Materials from Crosslinked Hydrogen-Bonded Columnar Liquid Crystals. *Adv. Mater. Interfaces* **2015**, *2*, 1500022.
(13) Marets, N.; Kuo, D.; Torrey, J. R.; Sakamoto, T.; Henmi, M.; Katayama, H.; Kato, T. Highly Efficient Virus Rejection with Self-Organized Membranes Based on a Crosslinked Bicontinuous Cubic Liquid Crystal. *Adv. Healthcare Mater.* **2017**, *6*, 1700252.
(14) Osada, I.; De Vries, H.; Scrosati, B.; Passerini, S. Ionic-Liquid-Based Polymer Electrolytes for Battery Applications. *Angew. Chem., Int. Ed.* **2016**, *55*, 500−513.
(15) Li, L.; Wu, Z.; Yuan, S.; Zhang, X.-B. Advances and Challenges for Flexible Energy Storage and Conversion Devices and Systems. *Energy Environ. Sci.* **2014**, *7*, 2101−2122.
(16) Sasi, R.; Chandrasekhar, B.; Kalaiselvi, N.; Devaki, S. J. Green Solid Ionic Liquid Crystalline Electrolyte Membranes with Anisotropic Channels for Efficient Li-Ion Batteries. *Adv. Sustainable Syst.* **2017**, *1*, 1600031.
(17) Lu, X.; Yu, M.; Wang, G.; Tong, Y.; Li, Y. Flexible Solid-State Supercapacitors: Design, Fabrication and Applications. *Energy Environ. Sci.* **2014**, *7*, 2160−2181.
(18) Sasi, R.; Sarojam, S.; Devaki, S. J. High Performing Biobased Ionic Liquid Crystal Electrolytes for Supercapacitors. *ACS Sustainable Chem. Eng.* **2016**, *4*, 3535−3543.
(19) Song, J. Y.; Wang, Y. Y.; Wan, C. C. Review of Gel-Type Polymer Electrolytes for Lithium-Ion Batteries. *J. Power Sources* **1999**, *77*, 183−197.
(20) Long, L.; Wang, S.; Xiao, M.; Meng, Y. Polymer Electrolytes for Lithium Polymer Batteries. *J. Mater. Chem. A* **2016**, *4*, 10038−10069.
(21) Stephan, A. M. Review on Gel Polymer Electrolytes for Lithium Batteries. *Eur. Polym. J.* **2006**, *42*, 21−42.
(22) Zhang, H.; Li, C.; Piszcz, M.; Coya, E.; Rojo, T.; Rodriguez-Martinez, L. M.; Armand, M.; Zhou, Z. Single Lithium-Ion Conducting Solid Polymer Electrolytes: Advances and Perspectives. *Chem. Soc. Rev.* **2017**, *46*, 797−815.
(23) Wright, P. V. Polymer Electrolytes—the Early Days. *Electrochim. Acta* **1998**, *43*, 1137−1143.
(24) Meyer, W. H. Polymer Electrolytes for Lithium-Ion Batteries. *Adv. Mater.* **1998**, *10*, 439−448.
(25) Croce, F.; Appetecchi, G. B.; Persi, L.; Scrosati, B. Nanocomposite Polymer Electrolytes for Lithium Batteries. *Nature* **1998**, *394*, 456−458.
(26) Pringle, J. M. Recent Progress in the Development and Use of Organic Ionic Plastic Crystal Electrolytes. *Phys. Chem. Chem. Phys.* **2013**, *15*, 1339−1351.
(27) Macfarlane, D. R.; Huang, J.; Forsyth, M. Lithium-Doped Plastic Crystal Electrolytes Exhibiting Fast Ion Conduction for Secondary Batteries. *Nature* **1999**, *402*, 792−794.
(28) Alarco, P.-J.; Abu-Lebdeh, Y.; Abouimrane, A.; Armand, M. The Plastic-Crystalline Phase of Succinonitrile as a Universal Matrix for Solid-State Ionic Conductors. *Nat. Mater.* **2004**, *3*, 476−481.
(29) Kato, T. From Nanostructured Liquid Crystals to Polymer-Based Electrolytes. *Angew. Chem., Int. Ed.* **2010**, *49*, 7847−7848.
(30) Yoshio, M.; Kato, T. Liquid Crystals as Ion Conductors. In *Handbook of Liquid Crystals*, 2nd ed.; Goodby, J. W., Collings, P. J., Kato, T., Tschierske, C., Gleeson, H., Raynes, P., Eds.; Wiley-VCH: Weinheim, 2014; Vol. *8*, pp 727−749.
(31) Cho, B.-K. Nanostructured Organic Electrolytes. *RSC Adv.* **2014**, *4*, 395−405.
(32) Wiesenauer, B. R.; Gin, D. L. Nanoporous Polymer Materials Based on Self-Organized, Bicontinuous Cubic Lyotropic Liquid Crystal Assemblies and Their Applications. *Polym. J.* **2012**, *44*, 461−468.
(33) Shimura, H.; Yoshio, M.; Hamasaki, A.; Mukai, T.; Ohno, H.; Kato, T. Electric-Field-Responsive Lithium-Ion Conductors of Propylenecarbonate-Based Columnar Liquid Crystals. *Adv. Mater.* **2009**, *21*, 1591−1594.
(34) Yoshio, M.; Mukai, T.; Ohno, H.; Kato, T. One-Dimensional Ion Transport in Self-Organized Columnar Ionic Liquids. *J. Am. Chem. Soc.* **2004**, *126*, 994−995.
(35) Ohtake, T.; Ogasawara, M.; Ito-Akita, K.; Nishina, N.; Ujiie, S.; Ohno, H.; Kato, T. Liquid-Crystalline Complexes of Mesogenic Dimers Containing Oxyethylene Moieties with $LiCF_3SO_3$: Self-Organized Ion Conductive Materials. *Chem. Mater.* **2000**, *12*, 782−789.
(36) Eisele, A.; Kyriakos, K.; Bhandary, R.; Schönhoff, M.; Papadakis, C. M.; Rieger, B. Structure and Ionic Conductivity of Liquid Crystals Having Propylene Carbonate Units. *J. Mater. Chem. A* **2015**, *3*, 2942−2953.
(37) Lee, J. H.; Han, K. S.; Lee, J. S.; Lee, A. S.; Park, S. K.; Hong, S. Y.; Lee, J.-C.; Mueller, K. T.; Hong, S. M.; Koo, C. M. Facilitated Ion Transport in Smectic Ordered Ionic Liquid Crystals. *Adv. Mater.* **2016**, *28*, 9301−9307.
(38) Ichikawa, T.; Yoshio, M.; Hamasaki, A.; Taguchi, S.; Liu, F.; Zeng, X.-b.; Ungar, G.; Ohno, H.; Kato, T. Induction of Thermotropic Bicontinuous Cubic Phases in Liquid-Crystalline Ammonium and Phosphonium Salts. *J. Am. Chem. Soc.* **2012**, *134*, 2634−2643.
(39) Soberats, B.; Yoshio, M.; Ichikawa, T.; Ohno, H.; Kato, T. Zwitterionic Liquid Crystals as 1D and 3D Lithium Ion Transport Media. *J. Mater. Chem. A* **2015**, *3*, 11232−11238.
(40) Kobayashi, T.; Ichikawa, T.; Kato, T.; Ohno, H. Development of Glassy Bicontinuous Cubic Liquid Crystals for Solid Proton-Conductive Materials. *Adv. Mater.* **2017**, *29*, 1604429.
(41) Yoshio, M.; Kagata, T.; Hoshino, K.; Mukai, T.; Ohno, H.; Kato, T. One-Dimensional Ion-Conductive Polymer Films: Alignment and Fixation of Ionic Channels Formed by Self-Organization of Polymerizable Columnar Liquid Crystals. *J. Am. Chem. Soc.* **2006**, *128*, 5570−5577.
(42) Kishimoto, K.; Suzawa, T.; Yokota, T.; Mukai, T.; Ohno, H.; Kato, T. Nano-Segregated Polymeric Film Exhibiting High Ionic Conductivities. *J. Am. Chem. Soc.* **2005**, *127*, 15618−15623.
(43) Ichikawa, T.; Yoshio, M.; Hamasaki, A.; Kagimoto, J.; Ohno, H.; Kato, T. 3D Interconnected Ionic Nano-Channels Formed in Polymer Films: Self-Organization and Polymerization of Thermotropic Bicontinuous Cubic Liquid Crystals. *J. Am. Chem. Soc.* **2011**, *133*, 2163−2169.
(44) Kerr, R. L.; Miller, S. A.; Shoemaker, R. K.; Elliott, B. J.; Gin, D. L. New Type of Li Ion Conductor with 3D Interconnected Nanopores via Polymerization of a Liquid Organic Electrolyte-Filled Lyotropic Liquid-Crystal Assembly. *J. Am. Chem. Soc.* **2009**, *131*, 15972−15973.
(45) Kerr, R. L.; Edwards, J. P.; Jones, S. C.; Elliott, B. J.; Gin, D. L. Effect of Varying the Composition and Nanostructure of Organic Carbonate-Containing Lyotropic Liquid Crystal Polymer Electrolytes on Their Ionic Conductivity. *Polym. J.* **2016**, *48*, 635−643.
(46) Högberg, D.; Soberats, B.; Uchida, S.; Yoshio, M.; Kloo, L.; Segawa, H.; Kato, T. Nanostructured Two-Component Liquid-Crystalline Electrolytes for High-Temperature Dye-Sensitized Solar Cells. *Chem. Mater.* **2014**, *26*, 6496−6502.
(47) Högberg, D.; Soberats, B.; Yatagai, R.; Uchida, S.; Yoshio, M.; Kloo, L.; Segawa, H.; Kato, T. Liquid-Crystalline Dye-Sensitized Solar Cells: Design of Two-Dimensional Molecular Assemblies for Efficient Ion Transport and Thermal Stability. *Chem. Mater.* **2016**, *28*, 6493−6500.
(48) Högberg, D.; Soberats, B.; Yoshio, M.; Mizumura, Y.; Uchida, S.; Kloo, L.; Segawa, H.; Kato, T. Self-Assembled Liquid-Crystalline

DOI: 10.1021/acsomega.7b01503
ACS Omega 2018, 3, 159−166

Ion Conductors in Dye-Sensitized Solar Cells: Effects of Molecular Sensitizers on Their Performance. *ChemPlusChem* **2017**, *82*, 834−840.
(49) Costa, R. D.; Werner, F.; Wang, X.; Grönninger, P.; Feihl, S.; Kohler, F. T. U.; Wasserscheid, P.; Hibler, S.; Beranek, R.; Meyer, K.; Guldi, D. M. Beneficial Effects of Liquid Crystalline Phases in Solid-State Dye-Sensitized Solar Cells. *Adv. Energy Mater.* **2013**, *3*, 657−665.
(50) Yamanaka, N.; Kawano, R.; Kubo, W.; Masaki, N.; Kitamura, T.; Wada, Y.; Watanabe, M.; Yanagida, S. Dye-Sensitized TiO_2 Solar Cells Using Imidazolium-Type Ionic Liquid Crystal Systems as Effective Electrolytes. *J. Phys. Chem. B* **2007**, *111*, 4763−4769.
(51) Abate, A.; Petrozza, A.; Cavallo, G.; Lanzani, G.; Matteucci, F.; Bruce, D. W.; Houbenov, N.; Metrangolo, P.; Resnati, G. Anisotropic Ionic Conductivity in Fluorinated Ionic Liquid Crystals Suitable for Optoelectronic Applications. *J. Mater. Chem. A* **2013**, *1*, 6572−6578.
(52) Kalhoff, J.; Eshetu, G. G.; Bresser, D.; Passerini, S. Safer Electrolytes for Lithium-Ion Batteries: State of the Art and Perspectives. *ChemSusChem* **2015**, *8*, 2154−2175.
(53) Goodenough, J. B.; Park, K.-S. The Li-Ion Rechargeable Battery: A Perspective. *J. Am. Chem. Soc.* **2013**, *135*, 1167−1176.
(54) Cook, J. B.; Kim, H.-S.; Lin, T. C.; Lai, C.-H.; Dunn, B.; Tolbert, S. H. Pseudocapacitive Charge Storage in Thick Composite MoS_2 Nanocrystal-Based Electrodes. *Adv. Energy Mater.* **2017**, *7*, 1601283.
(55) Kajiyama, S.; Szabova, L.; Iinuma, H.; Sugahara, A.; Gotoh, K.; Sodeyama, K.; Tateyama, Y.; Okubo, M.; Yamada, A. Enhanced Li-Ion Accessibility in MXene Titanium Carbide by Steric Chloride Termination. *Adv. Energy Mater.* **2017**, *7*, 1601873.
(56) Xu, K. Nonaqueous Liquid Electrolytes for Lithium-Based Rechargeable Batteries. *Chem. Rev.* **2004**, *104*, 4303−4418.
(57) Erickson, E. M.; Markevich, E.; Salitra, G.; Sharon, D.; Hirshberg, D.; de la Llave, E.; Shterenberg, I.; Rozenman, A.; Frimer, A.; Aurbach, D. Review—Development of Advanced Rechargeable Batteries: A Continuous Challenge in the Choice of Suitable Electrolyte Solutions. *J. Electrochem. Soc.* **2015**, *162*, A2424−A2438.
(58) Watanabe, M.; Thomas, M. L.; Zhang, S.; Ueno, K.; Yasuda, T.; Dokko, K. Application of Ionic Liquids to Energy Storage and Conversion Materials and Devices. *Chem. Rev.* **2017**, *117*, 7190−7239.
(59) Kato, Y.; Hori, S.; Saito, T.; Suzuki, K.; Hirayama, M.; Mitsui, A.; Yonemura, M.; Iba, H.; Kanno, R. High-Power All-Solid-State Batteries Using Sulfide Superionic Conductors. *Nat. Energy* **2016**, *1*, 16030.
(60) Blake, A. J.; Kohlmeyer, R. R.; Hardin, J. O.; Carmona, E. A.; Maruyama, B.; Berrigan, J. D.; Huang, H.; Durstock, M. F. 3D Printable Ceramic-Polymer Electrolytes for Flexible High-Performance Li-Ion Batteries with Enhanced Thermal Stability. *Adv. Energy Mater.* **2017**, *7*, 1602920.
(61) McGrogan, F. P.; Swamy, T.; Bishop, S. R.; Eggleton, E.; Porz, L.; Chen, X.; Chiang, Y.-M.; Van Vliet, K. J. Compliant Yet Brittle Mechanical Behavior of Li2S−P2S5 Lithium-Ion-Conducting Solid Electrolyte. *Adv. Energy Mater.* **2017**, *7*, 1602011.
(62) Tanibata, N.; Tsukasaki, H.; Deguchi, M.; Mori, S.; Hayashi, A.; Tatsumisago, M. Novel Discharge-Charge Mechanism of S-P_2S_5 Composite Electrode without Electrolyte in All-Solid-State Li/S Batteries. *J. Mater. Chem. A* **2017**, *5*, 11224−11228.
(63) Suzuki, Y.; Kami, K.; Watanabe, K.; Watanabe, A.; Saito, N.; Ohnishi, T.; Takada, K.; Sudo, R.; Imanishi, N. Transparent Cubic Garnet-Type Solid Electrolyte of Al_2O_3-Doped $Li_7La_3Zr_2O_{12}$. *Solid State Ionics* **2015**, *278*, 172−176.
(64) Sakuda, J.; Hosono, E.; Yoshio, M.; Ichikawa, T.; Matsumoto, T.; Ohno, H.; Zhou, H.; Kato, T. Liquid-Crystalline Electrolytes for Lithium-Ion Batteries: Ordered Assemblies of a Mesogen-Containing Carbonate and a Lithium Salt. *Adv. Funct. Mater.* **2015**, *25*, 1206−1212.
(65) Yoshio, M.; Mukai, T.; Kanie, K.; Yoshizawa, M.; Ohno, H.; Kato, T. Layered Ionic Liquids: Anisotropic Ion Conduction in New Self-Organized Liquid-Crystalline Materials. *Adv. Mater.* **2002**, *14*, 351−354.
(66) Shimura, H.; Yoshio, M.; Hoshino, K.; Mukai, T.; Ohno, H.; Kato, T. Noncovalent Approach to One-Dimensional Ion Conductors: Enhancement of Ionic Conductivities in Nanostructured Columnar Liquid Crystals. *J. Am. Chem. Soc.* **2008**, *130*, 1759−1765.
(67) Bouchet, R.; Maria, S.; Meziane, R.; Aboulaich, A.; Lienafa, L.; Bonnet, J.-P.; Phan, T. N. T.; Bertin, D.; Gigmes, D.; Devaux, D.; Denoyel, R.; Armand, M. Single-Ion BAB Triblock Copolymers as Highly Efficient Electrolytes for Lithium-Metal Batteries. *Nat. Mater.* **2013**, *12*, 452−457.
(68) Rohan, R.; Pareek, K.; Chen, Z.; Cai, W.; Zhang, Y.; Xu, G.; Gao, Z.; Cheng, H. A High Performance Polysiloxane-Based Single Ion Conducting Polymeric Electrolyte Membrane for Application in Lithium Ion Batteries. *J. Mater. Chem. A* **2015**, *3*, 20267−20276.
(69) Croce, F.; Sacchetti, S.; Scrosati, B. Advanced, Lithium Batteries Based on High-Performance Composite Polymer Electrolytes. *J. Power Sources* **2006**, *162*, 685−689.
(70) Porcarelli, L.; Shaplov, A. S.; Salsamendi, M.; Nair, J. R.; Vygodskii, Y. S.; Mecerreyes, D.; Gerbaldi, C. Single-Ion Block Copoly(ionic liquid)s as Electrolytes for All-Solid State Lithium Batteries. *ACS Appl. Mater. Interfaces* **2016**, *8*, 10350−10359.

DOI: 10.1021/acsomega.7b01503
ACS Omega 2018, 3, 159−166